ADJUSTABLE FLOW-CONTROL VALVE FOR THE SELF-ENERGISING ELECTRO-HYDRAULIC BRAKE

Michael Kuehnlein[1], Matthias Liermann[2], Julian Ewald[1] and Hubertus Murrenhoff[1]

[1]RWTH Aachen University, Institute for Fluid Power Drives and Controls (IFAS), Steinbachstr. 53, D-52074 Aachen, Germany
[2]American University of Beirut (AUB), Faculty of Engineering and Architecture (FEA), Riad El Solh, Beirut 1107 2020, Lebanon
Michael.Kuehnlein@ifas.rwth-aachen.de; Matthias.Liermann@aub.edu.lb.

Abstract

This paper presents the design and performance of an electrically adjustable flow control valve. It is designed specifically for the self-energising electro-hydraulic brake which requires small volume flows, a fail-safe open characteristic, a leakage tight closed position, simple control by just one solenoid, good dynamics, and repeatability.

The valve concept is based on a conventional pressure compensator design usually found in flow-control valves. The measuring orifice used to sense the flow through the valve is typically constant. In the presented design it is made adjustable using a hydro-mechanical pilot servo mechanism. The pilot is actuated by a proportional solenoid. The paper explains static flow equations used to parameterise the design. Dynamic simulation is used to validate the design before manufacturing. Measurements of the prototype show a good match with the simulation.

Measurements of the main characteristics of the valve are shown, specifically the dynamic response to a step input as well as the flow-signal tracking and load pressure disturbance rejection behaviour. The valve is also tested in its target application, the self-energising electro-hydraulic brake, where it proves its effectiveness in normalising the response time of the non-linear and the inherently unstable brake. As opposed to a non-linear or gain-scheduling control, with the new valve the controller of the brake can be designed as a simple switching control. This is an advantage for the overall brake's safety evaluation and therefore helps to improve the prospects of using the self-energising brake in future applications such as rail vehicles.

Keywords: hydraulic brake, self-energising, brake torque control, leakage-free adjustable flow-control valve, flow-control valve, integrated valve

1 Introduction

Hydraulic brakes have been designed for railway vehicles in the past (Hommen, 1986). They offer high power-density (Murrenhoff, 2011) and are therefore dedicated to meet the strict installation space requirements present in railed vehicles. Conventional hydraulic friction brakes use a hydraulic power-pack to provide the clamping energy. To reduce the power consumption self-energising principles are promising. The Self-Energising Electro-Hydraulic Brake (SEHB) was developed at RWTH Aachen University, Institute for Fluid Power Drives and Controls (IFAS). It combines the advantages of high power-density and reduced power consumption (Liermann, 2008; Ewald, 2011).

The SEHB uses the kinetic energy of the vehicle as a source of energy to produce its clamping force. Electrical power is only needed on a signal level for valve actuation (Ewald et al., 2008). Figure 1 shows a schematic of the developed Self-energising Electro-Hydraulic Brake. The brake mainly consists of the brake pads, a calliper, a brake actuator, a supporting cylinder, and control valves.

To describe its functionality, a braking process shall be considered: The piston side chamber of the brake actuator is pressurised, causing the brake actuator to move outwards and thereby clamping the brake pads onto the brake disc via the calliper. The depicted guidance allows for a movement of the whole calliper, including the brake actuator and the brake pads, in tangential direction of the brake disc. As can be seen in the lower view of Fig. 1, the supporting cylinder is mounted to the calliper and its rod is fixed to the vehicle chassis.

The tangential movement of the brake calliper is limited by the supporting cylinder. As the calliper

This manuscript was received on 30 October 2011 and was accepted after revision for publication on 4 March 2012

moves, it induces a load for the supporting cylinder and hydraulic pressure builds-up in the chamber of the supporting cylinder. The piston area of the supporting cylinder is chosen in such a way that during the braking process the pressure in its chamber is always higher than the hydraulic pressure in the brake actuator piston side chamber.

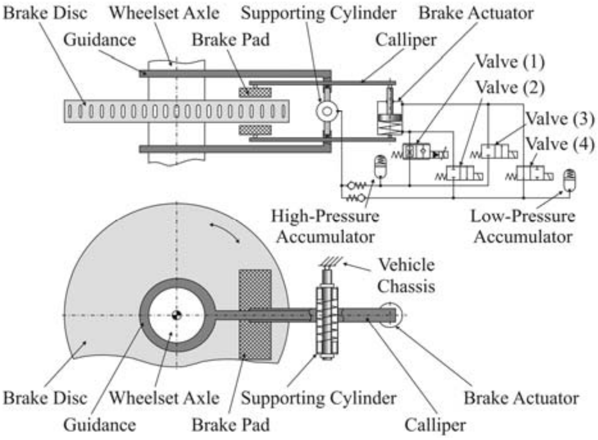

Fig. 1: *Schematic of the Self-energising Electro-Hydraulic Brake*

If all control valves are de-energised the chamber of the supporting cylinder is connected to the piston side chamber of the brake actuator. This leads to a pressure increase in the brake actuator piston side chamber. The higher clamping force causes a higher pressure in the supporting cylinder and so the loop of self-energisation is closed. Closing all control valves keeps the clamping force constant. Connecting the brake actuator piston side chamber to the low pressure line reduces the clamping force.

The pressure in the supporting cylinder is proportional to the tangential brake force. The brake torque is a product of friction radius and tangential brake force. As the friction force is kept constant the supporting cylinder pressure is proportional to the brake torque. The control of the supporting cylinder pressure therefore facilitates a control of the brake torque.

During the brake torque build-up the braking process is unstable without control (Liermann, 2008). This means that the brake force is increasing with a progressive dynamics. Therefore, a higher brake force level corresponds to a larger jerk of the train if only a simple proportional control is applied (Ewald, 2011). Due to comfort requirements the jerk during braking is limited (BS EN 13452, 2003). To ensure the demands are met the brake force build-up should be the same, no matter if the reference brake force is high or low. With the SEHB, this can be achieved only if the brake dynamics, which increase with brake force level, are linearised either by a non-linear feedback on signal level (Kuehnlein et al., 2011) or with hydro-mechanical control measures inherently implemented in the physical design. The latter is the approach of this paper using an adjustable flow-control valve tailored specifically for the SEHB.

2 Performance Requirements and Concept

As the valve is designed for the SEHB the requirements which arise from the brake system need to be fulfilled. At the end of the chapter the valve prototype meeting the demands for a constant flow is shown. The next paragraph answers the question why a constant flow is necessary.

2.1 Constant Volume Flow

The brake force build-up $\dot{F}_{\mathrm{Brake}}$ is proportional to the clamping pressure build-up $\dot{p}_{\mathrm{A}}$ in the brake actuator piston side chamber. The pressure build-up equation of the brake actuator piston side chamber is (Murrenhoff, 2011),

$$\dot{p}_{\mathrm{A}} = \frac{1}{C_{\mathrm{H,A}}}\left(Q_{\mathrm{V}} - Q_{\mathrm{BA}}\right) \tag{1}$$

where $C_{\mathrm{H,A}}$ is the capacity, Q_{V} the valve flow, and Q_{BA} the flow due to the motion of the cylinder. When the brake is clamped this movement is negligible. The progression of the brake force build-up is desired to be linear, resulting in a constant pressure build-up requirement. Therefore, the volume flow to the brake actuator piston side chamber should be kept constant during brake force build-up.

In the case of the SEHB the pressure in the supporting cylinder p_{SC} increases when the loop of self-energisation is closed which results in rising pressure difference available for the control valve. Spool valves have an increasing volume flow due to the rising pressure difference which can be calculated by the orifice equation (Murrenhoff, 2011). As pointed out, a constant volume flow independent of the pressure difference is needed which can be achieved with flow-control valves.

2.2 Demands of the SEHB

Besides the requirement of a constant volume flow independent of the pressure difference there are additional demands for the control valve. The valve needs to be leakage free to avoid high-pressure oil being drained when the brake is not in operation. To allow for a fail-safe function of the SEHB it is required to be of normally open type. Another important design target is the maximum volume flow.

The brake's maximum clamping force F_{BA} is 32000 N which should be reached within a minimum time t of 1 s. The railway standard for brakes (BS EN 13452, 2003) requires that the force is build-up within a maximum time limit of 4 s. The purpose of this standard is to limit the maximum jerk in different braking situations for passenger comfort and safety. However, higher dynamics is required to perform slip control action. For this reason the requirement for the brake valve of the SEHB is chosen to be four times faster than the limit given in the standard. With the cylinder's equation of motion the clamping force F_{BA} is calculated from the pressure in the piston side chamber p_{A} multiplied with the corresponding Area A_{A} and the pressure in the ring side chamber p_B multiplied by the piston side area A_B, when the spring force and the cylinder mass is neglected.

$$F_{BA} = p_A A_A - p_B A_B \tag{2}$$

During brake force build-up p_B is constantly at 2.7 bar. With the piston area A_A (5027 mm²) and the ring area A_B (2651 mm²) the pressure p_A which is corresponding to the maximum clamping force is 65 bar. Considering the desired time t and assuming a linear progression of the force build-up the pressure gradient $\dot{p}_A$ is 65 bar/s. Considering Eq. 1 and expressing the flow due to the brake actuator motion with the cylinder velocity $\dot{x}_{BA}$ and the piston side area A_A yields Eq. 3.

$$\dot{p}_A = \frac{1}{C_{H,A}}\left(Q_V - A_A \dot{x}_{BA}\right) \tag{3}$$

The hydraulic capacity $C_{H,A}$ has a value of $8.78 \cdot 10^{-14}\ \mathrm{m^3/Pa}$ and the velocity of the cylinder movement $\dot{x}_{BA}$ is approximated by 2.7 mm/s, which is based upon data obtained from a full braking measurement. Considering the calculated pressure gradient leads to a valve flow Q_V of 0.85 l/min.

Therefore, the design is aimed at a maximum volume flow of 0.85 l/min. Furthermore, the flow needs to be continuously adjustable to facilitate tuneable dynamics of the brake force build-up.

The summarised requirements for the SEHB control valve are

- Leakage free
- Maximum volume flow 0.85 l/min
- Normally open (NO)
- Flow control function
- Adjustable volume flow during brake operation
- One electromechanical converter

Various adjustable flow control valves are available on the market. Moreover, even valves with an integrated closed position are offered. They allow a maximum volume flow of 100 l/min (Linden, 2007) and 25 l/min (Roth, 2010) respectively. If valves of such a high flow are used for the SEHB a switching control could not be applied as the brake force build-up and the resolution for small volume flows would not be appropriate. Moreover, both valves (Linden, 2007; Roth, 2010) are typically used for load holding applications and are therefore normally closed (NC) which means they are not suitable for the safety concept of the SEHB. Consequently, a valve meeting the demands is designed which concept is discussed next.

2.3 Valve Concept

Flow control valves consist mainly of a pressure compensator and a measuring orifice. The pressure of the supporting cylinder changes fast and hence a valve with a downstream pressure compensator is preferred (Murrenhoff, 2011). The principle of the required valve is shown in Fig. 2. It mainly consists of a pressure compensator and a measuring orifice. The measuring orifice is adjustable to allow a regulation of the volume flow set point. To reduce the pressure dependency for operation of the measuring orifice it is piloted. In the following the realisation of four main functions of the valve is explained:

- pressure compensated flow control,
- adjustability of flow control,
- servo-hydraulic pilot stage which sets the measuring orifice opening,
- leakage tightness.

Pressure Compensated Flow Control

The pressure compensator has two face side areas $A_{C,Piston}$ which are identical in size. The area on the right hand side is connected with the *inlet port* via a line that runs through *main seat 2*, whereas the area to the left is connected to a volume in which the pressure $p_{Control}$ is present. The pressure $p_{Control}$ equals the inlet pressure p_{In} minus the pressure drop across the *measuring orifice*. Furthermore, a spring is mounted to the left hand side of the *pressure compensator* which acts in opening direction. The hydraulic resistance of the main seat is small compared to the measuring orifice. Therefore, the pressure compensator spool area on the left hand side is exposed to the pressure behind the measuring orifice and the area on the right hand side is exposed to the inlet pressure.

If static operation with a constant volume flow through the *outlet port* is considered, the pressure drop across the measuring orifice is constant. If the pressure at the outlet is constant and the inlet pressure suddenly increases, the volume flow would increase if the pressure compensator's opening area was constant. With the rise of the inlet pressure the pressure regulator decreases its opening area and so the volume flow is reduced and kept at the previous level.

Adjustability of Flow Control

The adjustability of the volume flow is accomplished by altering the opening of the measuring orifice which results in a change of the measuring orifice pressure drop. This influences the balance of forces of the pressure compensator directly, namely the pressure exerted to the left face side. As the spring of the pressure compensator establishes the proportionality between force and position, the opening area is affected.

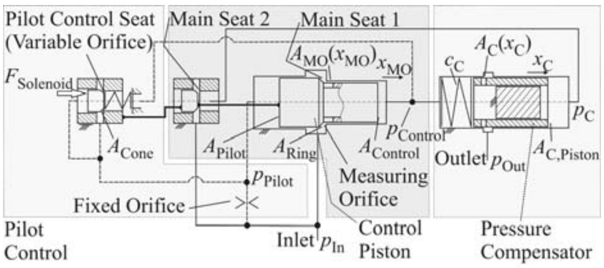

Fig. 2: *Functional diagram of the flow-control valve*

Servo-Hydraulic Pilot Stage

To keep the influence of the flow forces at a minimum, the servo-hydraulic pilot stage is needed. The motion of the *control piston* varies the opening area of the measuring orifice. The control piston has two face side areas ($A_{Control}$ and A_{Pilot}) and one ring area (A_{Ring}). The area A_{Pilot} is pressurised with pilot pressure p_{Pilot}. It is controlled by a pressure divider which consists of a *fixed orifice* to inlet pressure p_{In} and a *variable orifice*, the *pilot control seat*. The pilot control seat connects to the pressure behind the measuring orifice $p_{Control}$. By the combination of fixed and variable orifice the pilot pressure is made a function of the pilot cone and control piston position. It can vary between inlet pressure (closed pilot) and $p_{Control}$ (fully opened pilot). The right side of the control piston is pressurised with p_{In} on area A_{Ring} and $p_{Control}$ on area $A_{Control}$. The pressure $p_{Control}$ is also controlled by a pressure divider consisting of a fixed and a variable orifice. The fixed orifice is the measuring orifice. Even though it is adjustable, it can be considered fixed because the purpose of the pilot stage is to control its position despite of other influences. The variable orifice is the outlet orifice of the pressure compensator stage.

The pilot is directly actuated by a proportional solenoid (not depicted). Closing the pilot orifice leads to an increase of the pressure p_{Pilot} and thus the cross sectional flow area of the measuring orifice A_{MO} in the control piston is reduced. Vice versa, opening the pilot reduces the pressure drop of the variable pilot orifice, leading to a decrease of the pressure p_{Pilot}. Thereby, the cross sectional flow area of the measuring orifice A_{MO} in the control piston is increased. Summing up, pilot control and control piston constitute a servo control.

Leakage Tightness

The proportional solenoid is a push type and closes the pilot when energised. The energised solenoid presses the pilot into its seat and the pilot housing is also moveable. This housing is mechanically connected to the main seat 2 and the control piston. Subsequently, closing the pilot simultaneously closes *main seat 1* and main seat 2. All flow paths to the pressure compensator need to be inhibited as the pressure compensator is a sleeve and therefore leakage is inherent. The direct flow from the inlet to the pressure compensator is blocked by main seat 1. Main seat 2 is necessary to prevent a flow to the right face side of the pressure compensator. The pilot flow is blocked by the pilot itself. It is also clear that the volume flow in closed position can not be ideally zero as the seals are metal to metal (Schmidt, 2010). In the next chapter the realised valve prototype is shown.

2.4 Valve Prototype

The valve is designed as a screw-in type and a sectional view is depicted in Fig. 3. A groove supplies the high pressure side of the pressure compensator with inlet pressure. This enables the main seats (compare Fig. 2) to be integrated into a single seat which in open position constitutes the measuring orifice. Furthermore, the fixed orifice for the piloting circuit is integrated into the control piston. The pilot piston ends cone-shaped. In combination with the seat in the control piston it constitutes the variable pilot orifice. If the solenoid is off, the pilot spring opens the variable pilot orifice. Energising the solenoid causes the pilot piston to be pushed into its seat in the control piston. Thereby, the control piston is also pushed into its seat and so the measuring orifice is closed.

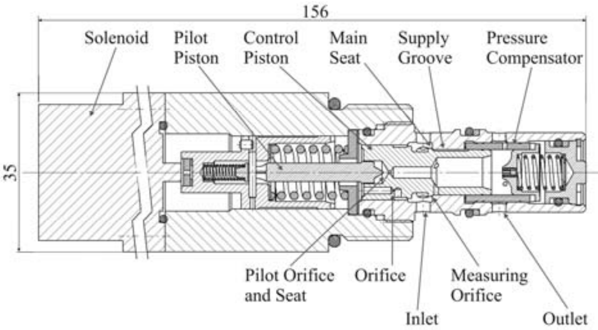

Fig. 3: *Sectional view of flow regulator valve*

In Fig. 4 the prototype is shown for which a proportional solenoid with a position transducer is used. The position transducer is useful for valve tests to monitor the pilot movement. For later application a solenoid without position transducer is intended. The employed solenoid is a Magnet-Schultz product, type GRFY035F20B61, with a nominal current of 680 mA and a nominal voltage of 24 V DC.

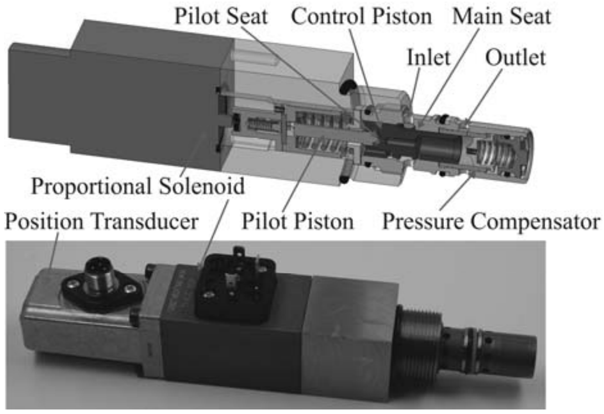

Fig. 4: *Valve prototype*

3 Static and Dynamic Characteristics of Valve

In this chapter the valve dimensioning is discussed, the system simulation model is shown, and the obtained experimental results are analysed.

3.1 Dimensioning Based on Static Equations

As the valve concept is determined the valve is dimensioned for which the static flow is calculated first. The flow through the pressure compensator Q_C is described with the orifice equation in which $\alpha_{D,C}$ is the flow coefficient, $A_C(x_C)$ the compensator opening area, ρ the fluid density, $p_{Control}$ the control pressure, and p_{Out} the outlet pressure.

$$Q_{\mathrm{C}} = \alpha_{\mathrm{D,C}} \cdot A_{\mathrm{C}}(x_{\mathrm{C}}) \cdot \sqrt{\frac{2}{\rho}\left(p_{\mathrm{Control}} - p_{\mathrm{Out}}\right)} \tag{4}$$

Radial holes in the pressure compensator constitute the opening area A_{C}. The opening area depends on the number of holes z, their radius r, and the compensator position x_{C}.

$$A_{\mathrm{C}}(x_{\mathrm{C}}) = z\left(r^2 \arccos\left(1 - \frac{x_{\mathrm{C}}}{r}\right) - \sqrt{2rx_{\mathrm{C}} - x_{\mathrm{C}}^2}\,(r - x_{\mathrm{C}})\right) \tag{5}$$

The flow through the measuring orifice Q_{MO} with its opening area $A_{\mathrm{MO}}(x_{\mathrm{MO}})$ with the flow coefficient $\alpha_{\mathrm{D,MO}}$ and the inlet pressure p_{In} is

$$Q_{\mathrm{MO}} = \alpha_{\mathrm{D,MO}} \cdot A_{\mathrm{MO}}(x_{\mathrm{MO}}) \cdot \sqrt{\frac{2}{\rho}\left(p_{\mathrm{In}} - p_{\mathrm{Control}}\right)} \tag{6}$$

When the pilot volume flow Q_{Pilot} is neglected the flow of the pressure compensator Q_{C} and the measuring orifice Q_{MO} is equal, the valve flow Q_{Valve} is

$$Q_{\mathrm{Valve}} = Q_{\mathrm{C}} = Q_{\mathrm{MO}} \tag{7}$$

Solving Eq. 6 for p_{Control} yields the pressure p_{Control}

$$p_{\mathrm{Control}} = p_{\mathrm{In}} - \frac{Q_{\mathrm{MO}}^2}{\alpha_{\mathrm{D,MO}}^2 \cdot \left(A_{\mathrm{MO}}(x_{\mathrm{MO}})\right)^2}\frac{\rho}{2} \tag{8}$$

When inserting Eq. 8 into Eq. 4 the flow Q_{C} is

$$Q_{\mathrm{C}} = \sqrt{\left(p_{\mathrm{In}} - \frac{Q_{\mathrm{MO}}^2}{\alpha_{\mathrm{D,MO}}^2 \cdot \left(A_{\mathrm{MO}}(x_{\mathrm{MO}})\right)^2}\frac{\rho}{2} - p_{\mathrm{Out}}\right)} \times \\ \times \alpha_{\mathrm{D,C}} \cdot A_{\mathrm{C}}(x_{\mathrm{C}})\sqrt{\frac{2}{\rho}} \tag{9}$$

Solving Eq. 9 for Q_{C} and with Eq. 7 the static volume flow of the valve is

$$Q_{\mathrm{Valve}} = \frac{\sqrt{\frac{2}{\rho}\cdot\left(p_{\mathrm{In}} - p_{\mathrm{Out}}\right)}}{\sqrt{\frac{1}{\left(\alpha_{\mathrm{D,C}} \cdot A_{\mathrm{C}}(x_{\mathrm{C}})\right)^2} + \frac{1}{\left(\alpha_{\mathrm{D,MO}} \cdot A_{\mathrm{MO}}(x_{\mathrm{MO}})\right)^2}}} \tag{10}$$

With this formula the dimensioning of the valves volume flow is accomplished. Due to the non-linear equations it is not possible to transform the system of equations to a form of $Q = f((p_{\mathrm{In}} - p_{\mathrm{Out}}), x_{\mathrm{C}})$ (Trudzinski, 1980). Hence, the calculation discretised. In a first step the measuring orifice opening area A_{MO} is fixed to its maximum. Then discrete positions of the pressure compensator spool x_{C} are given and the pressure compensator opening area A_{C} is calculated for all positions x_{C} with Eq. 5. With this information the pressure difference $p_{\mathrm{In}} - p_{\mathrm{Out}}$ is calculated for each pressure compensator position and so all values of Eq. 10 are known and the volume flow is calculated. This procedure is repeated for other discrete measuring orifice opening area values A_{MO}. The parameter values for the fully opened valve are listed in Table 1.

Table 1: Design parameters for static dimensioning

Parameter	Value [Unit]
$A_{\mathrm{MO}}(x_{\mathrm{MO}})$	1.148 [mm²]
r	0.45 [mm]
z	3 [-]
$\alpha_{\mathrm{D,C}}$	0.65 [-]
$\alpha_{\mathrm{D,MO}}$	0.65 [-]
ρ	835.3 [kg/m³]

The resulting maximum flow for full opening area A_{MO} dependent on the pressure difference $\Delta p = p_{\mathrm{In}} - p_{\mathrm{Out}}$ is illustrated in Fig. 5.

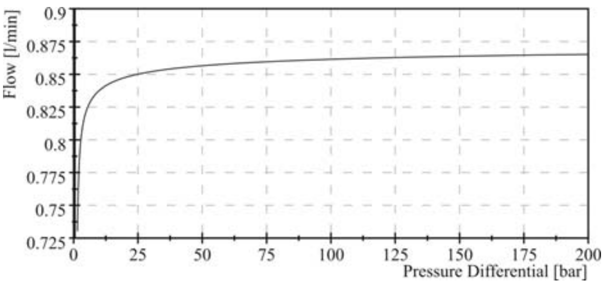

Fig. 5: *Calculated valve flow Q_{Valve} with regard to pressure difference*

For maximum measuring orifice opening A_{MO} with de-energised solenoid the valve flow is limited to 0.86 l/min and a pressure difference of 3 bar is needed to reach a flow of 0.80 l/min. As can be seen from the plot, the valve shows good disturbance rejection with regard to Δp .

3.2 Dynamic Simulation

To verify the functionality dynamically a system simulation model of the valve is set up with DSH*plus*. An overview of this model is shown in Fig. 6.

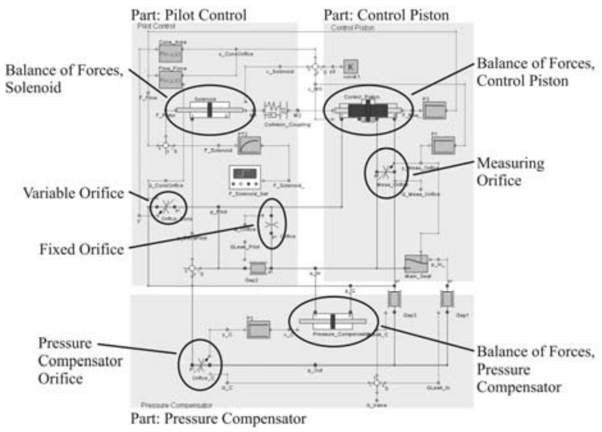

Fig. 6: *Simulation model of developed valve*

The simulation model consists of the three main valve parts which are the pressure compensator, the control piston, and the pilot control. Integral element of each part is an adjustable orifice. In the model the opening of each of these orifices is determined by a balance of forces within a cylinder. In the case of the control piston a cylinder with three areas is used and its position is the input of the measuring orifice opening. Besides the areas and the springs, cylinder masses and viscous damping is parameterised. To account for the dynamics of the solenoid a first order lag element is included. The pilot piston is realised as a cone element and therefore the flow force F_{Flow} is included. It is calculated with the fluid density ρ, the fluid velocity $\dot{x}_{\text{Fluid}}$, the flow Q, and the flow angle ε (Murrenhoff, 2011)

$$F_{\text{Flow}} = \rho \cdot \dot{x}_{\text{Fluid}} Q \cos \varepsilon \tag{11}$$

The velocity of the fluid in the gap is expressed by the continuity equation. Thus, the flow force in the simulation model is determined by Eq. 12, where $A_{\text{Cone}}(x_{\text{Cone}})$ describes the cone shaped opening area

$$F_{\text{Flow}} = \frac{\rho \cdot Q^2}{A_{\text{Cone}}(x_{\text{Cone}})} \cos \varepsilon \tag{12}$$

In addition the gap leakage of the pressure compensator and the control piston is considered. Simulation results compared to measurement results are presented in the next two chapters.

3.3 Experimental Validation

To validate the static volume flow as well as the dynamic response, the valve is examined experimentally on a valve test rig built-up for this purpose. The schematic of the hydraulic test circuit is illustrated in Fig. 7 which is according to (ISO 6403, 1992). The volume flow is measured with a flowmeter and in addition a measuring orifice is added for dynamic volume flow sensing. To validate the step response of the test valve the ball valve is kept closed and the servo valve is opened.

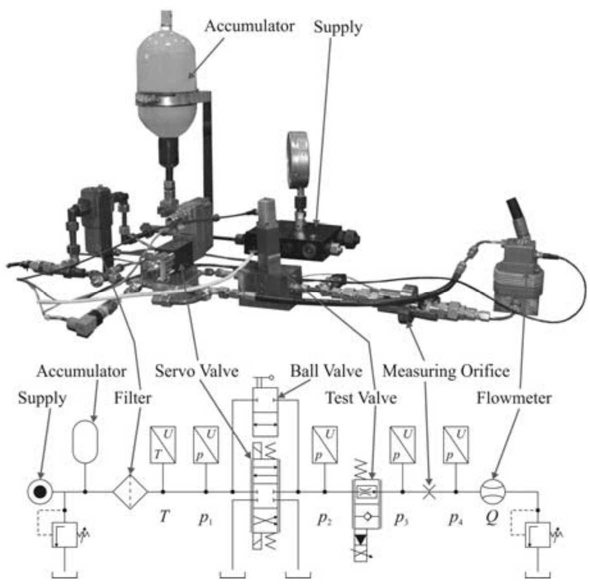

Fig. 7: *Test circuit for designed valve*

By applying a pressure ramp to p_2 the flow rate characteristic dependent on the pressure drop across the test valve is determined. For this purpose the ball valve is opened and the servo valve performs a bypass control of the pressure p_2.

In Fig. 8 the response to a signal step from 0% to 74% of the nominal current is depicted. Before the signal rise the flow is 0.85 l/min. The valve has a constant flow of 0.38 l/min during the signal increase. After the signal is set back to 0% (0 mA) a flow of 0.85 l/min is reached again. It should be noted that the valve reacts with a delay $t_{\text{d,s}}$ of 178 ms to the increasing signal step and then needs a time $t_{\text{a,s}}$ of 168 ms to adjust to the set value. At the decreasing signal step the valve reacts after $t_{\text{d,e}}$ 37 ms. A flow of 0.8 l/min is reached within an adjustment time $t_{\text{a,e}}$ of 486 ms. These fairly large time delays are due to friction and viscous damping especially in the pilot stage of the valve which is identified by simulation. The valve reaction time can be reduced with over-excitation of the solenoid and increased radial clearance of the auxiliary pilot piston.

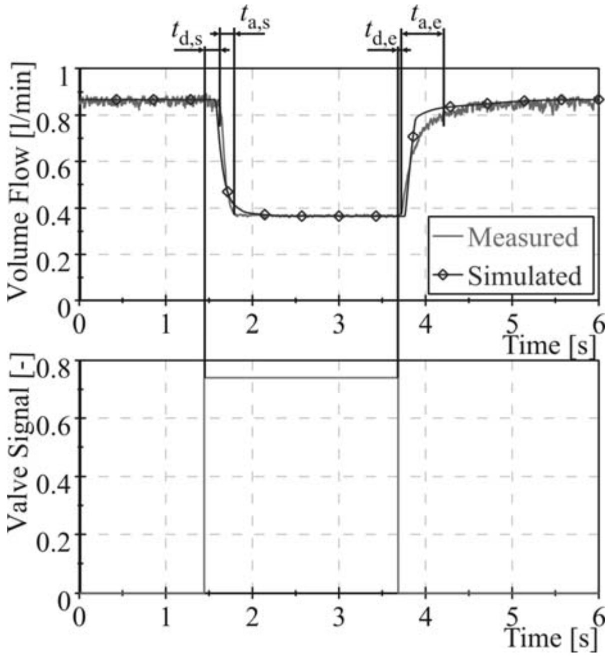

Fig. 8: *Signal step response of measurement and simulation*

Valve signal and supply pressure ramps are applied to determine the flow-signal plot and the flow-pressure differential characteristic illustrated in Fig. 9. The flow measured by the measuring orifice is altered between a valve signal of 70 % and 77 % of the nominal current. It has a signal hysteresis of about 1 % with regard to the nominal current and 17 % with regard to the full control range. In the upper plot of Fig. 9 the pressure difference is 90 bar. The steps during opening are explained by the breakaway friction force of the pilot (at 74.7 %) and the control piston (at 73 %). The minimum flow is 0.028 l/min, which is higher than values of conventional seat-type valves (Sterling Hydraulics, 2011). It can be optimised e.g. with a soft seat and will be reduced in future improvement.

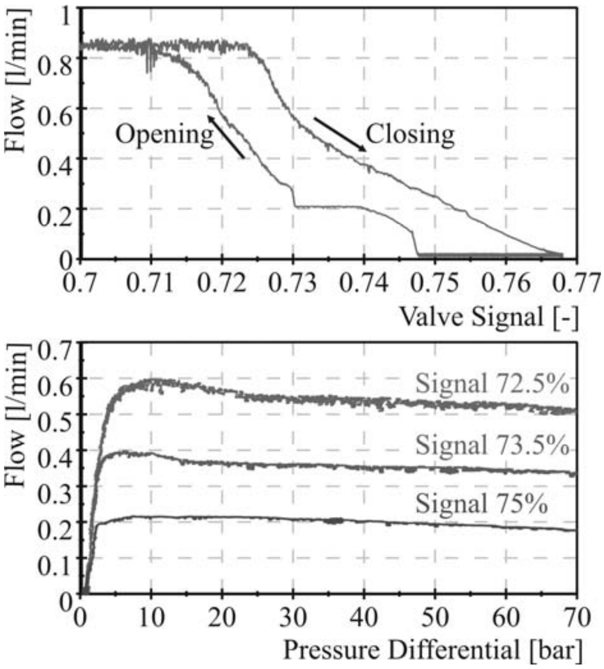

Fig. 9: *Flow-signal and flow-pressure differential characteristics*

The lower plot of Fig. 9 depicts the static characteristics of the designed valve, which are shown for valve closing. A pressure difference of 2 bar (75 %) to 6 bar (72.5 %) is necessary to overcome the spring pre-load of the pressure compensator. In the working range of the flow-control valve the characteristic curves show a negative slope which is caused by the dominance of the flow force at the pressure compensator when compared to the pressure compensator spring force (Murrenhoff, 2011).

As the characteristics of the valve are determined the valve is applied to the SEHB test rig in a next step.

4 Brake Performance with Adjustable Flow-Control Valve

This chapter presents the brake test rig and experimental results acquired with the designed valve.

4.1 SEHB Test Rig

The test bench mainly consists of the SEHB, the driving unit, and the signal processing equipment. A front view of the test rig is shown in Fig. 10. The railway brake disc with a diameter of 640 mm is mounted on a shaft with two clamping sets. The shaft itself is fixed to the T-slot test bed with spherical roller bearings. Each end of the brake disc shaft is connected via a jaw-type clutch to a hydraulic axial piston motor. Those two driving axial piston motors have a compression volume of 250 cm³ each and are supplied by a central pressure supply unit.

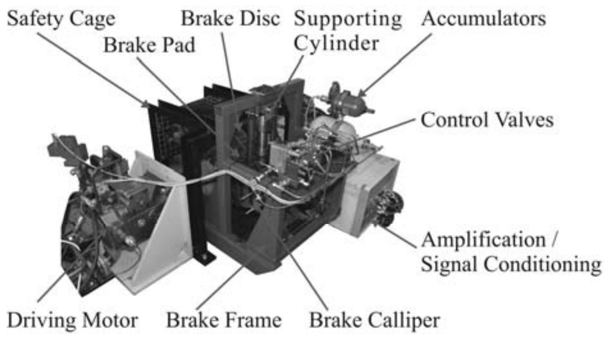

Fig. 10: *SEHB test rig*

The brake is mounted on a frame to the test bed. Accumulators and the control valve are mounted to the brake frame. In Fig. 10 the brake calliper, the supporting cylinder, and the amplification and signal conditioning equipment can be seen. dSPACE real-time hardware is used to process the test rig signals to the measurement computer and also to send command signals to the control valve.

Besides the left driving motor and the brake with the brake actuator, the safety cage for the brake disc is illustrated. With this SEHB test rig the experiments are carried out.

4.2 Measurement Results

The developed valve, designated as valve (1), is mounted to the SEHB system according to the hydraulic schematic depicted in Fig. 1. It controls the flow from the high pressure line towards the piston side chamber of the brake actuator during brake force increase. During the presented results in this paper valves (2), (3), and (4) (see Fig. 1 for reference) are in closed position for the shown brake force build-up. For brake force decrease valve (1) is kept closed and valve (2), which connects the brake actuator piston side chamber and the low pressure line, is opened. A switching control is applied in which the opening signal is constant during one experiment. The controller is set up in Matlab Simulink that controls the SEHB and the brake disk drive. The Simulink model is executed by a dSPACE real-time hardware with a sampling frequency of 2.9 kHz. Assuming low friction in piston sealings, the brake force of the SEHB is proportional to the pressure in the supporting cylinder irrespective of the brake friction coefficient (cf. Liermann, 2008). Therefore, the supporting cylinder pressure is measured as the control variable. As supporting cylinder pressure and brake force are in proportional relation, for means of clarity the brake force is discussed in the following. To increase the brake force valves (2), (3), and (4) are kept closed and valve (1) is opened. If the desired brake force level is reached, which is detected by the supporting cylinder pressure, valve (1) is closed.

The upper plot of Fig. 11 shows the step response for a brake force step from 3000 N to 6000 N with a valve signal of 72.25 % of the nominal current. The time for the brake force build-up is 0.94 s and was expected by simulation. After the brake force reaches the desired value of 6000 N it is oscillating in a triangular shape. This oscillation is due to a varying friction coefficient between brake pad and brake disc, which directly influences the proportional relation between supporting cylinder pressure and brake force calculation. The lower diagram of Fig. 11 depicts the step response for various constant valve signals. Main aim of the developed valve is to be able to vary the time for the brake force increase. During each of the shown experiments in the lower plot of Fig. 11 the valve signal values are kept constant at the given values between 0 s and 3 s. Applying 74.5 % of the nominal current to the solenoid leads to a rise time of 1.54 s. With maximum valve opening the time for brake force build-up is reduced to 0.27 s, allowing good slip control. The whole range of brake force dynamics is within the time specifications given in the respective railway standard, which limits the time for brake force build-up to 4 s (BS EN 13452, 2003).

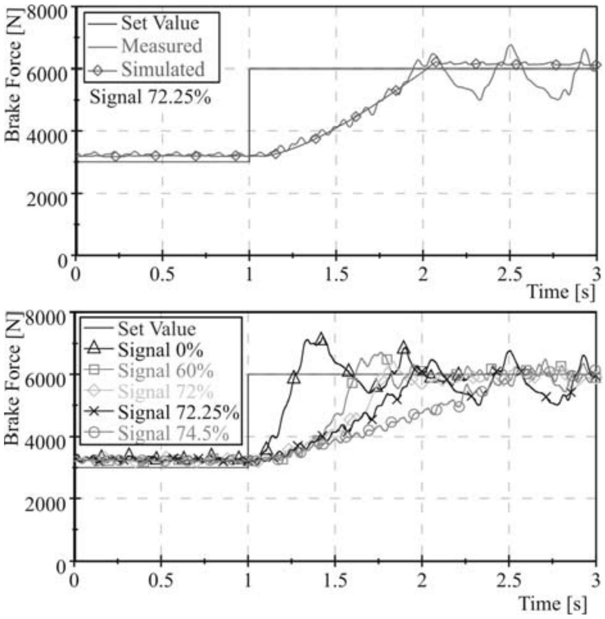

Fig. 11: *Experimental results obtained with designed valve in SEHB*

The brake force response curves for valve set-point values between 72 % and 74.5 % are very similar in the first 300 ms as the lower plot of Fig. 11 shows. This is due to the delayed reaction of the valve pilot stage and the subsequent movement of the control piston. This behaviour was anticipated from the analysis of the valve step response experiments shown in Fig. 8. After the valve has reached its control position, the different dynamics are well distinguished and correspond to the valve set value. Using this novel valve the brake force build-up can be adjusted while the flow-control functionality linearises the brake force dynamics. This is a huge advantage compared to regular flow-control valves which require an electronic closed loop spool position control and signal based gain scheduling control to achieve the same task, which is to achieve a predictable and similar jerk for every brake force level. The valve presented in this paper uses only a simple switching control resulting in the use of a cost-effective brake controller similar to existing brake controllers for state-of-the-art pneumatic railway brakes. This facilitates the straightforward integration into current railway brake infrastructure.

5 Conclusion

We developed a leakage-free adjustable flow-control valve for the SEHB for railway applications. The valve facilitates a linearised brake force build-up to achieve predictable vehicle jerk by maintaining a constant flow during brake force increase. Due to the inherent control function of the valve, it is possible to operate the brake with pure switching control, which is required for fail-safe scenarios. The valve comprises a pressure compensator to keep the flow constant regardless of the pressure difference. The measuring orifice is designed adjustable which is accomplished by a moveable control piston. The control piston is pilot operated by a simple servo-hydraulic mechanism driven by a proportional solenoid. In off position the valve is open to accommodate the safety concept of the SEHB. The valve is designed as a seat-type valve. It is therefore technically leakage-free in closed position. For static operation the flow is limited to 0.85 l/min.

With a valve test assembly the functionality is validated. It shows good adjustability of the flow, the expected maximum flow is 0.85 l/min and it has an acceptable hysteresis of 17 %. This hysteresis is acceptable as a look-up table with the hysteresis information can be given to the brake controller. For a step of the valve input signal the flow adjusts to the desired value with a time delay of 178 ms. For constant valve signal the flow remains constant for a wide load pressure range. In closed position the valve has a minimum flow of 0.028 l/min which is higher than conventional seat-type valves but will be reduced in a future re-design.

The versatility of the valve for use with the SEHB is shown on a full-scale railway brake test rig for the self-energising brake system. The achieved brake force build-up dynamics are widely linear and show very good match with our simulation. For a step of the brake force from 3000 N to 6000 N the brake response time can be regulated from 0.27 s to 1.54 s by adjusting the valve input signal. These values comply well with requirements set in railway brake standards.

The conclusion we draw is that the developed valve is suitable for operation with the SEHB as it works reliably with switching control for fail-safe scenarios but can also be adjusted to realise comfort functions with a simple electronic open-loop current driver stage. The electronic circuits for this purpose are simple enough that they can be realised with the required safety-level and durability for the harsh conditions in a railway undercarriage. Existing brake controllers for state-of-the-art pneumatic railway brakes can be adapted for use with the self-energising electro-hydraulic brake.

Acknowledgements

The authors express their thanks to the German Research Foundation (DFG) for funding the research on the SEHB. Further thanks go to Magnet-Schultz GmbH & Co. KG and Bucher Hydraulics AG for providing the authors with components.

Nomenclature

A	Constant for valve dimension	[mm²]
A_A	Brake actuator piston side area	[mm²]
A_B	Brake actuator ring side area	[mm²]
$A_C(x_C)$	Pressure compensator area, dependent on position	[mm²]
A_{Cone}	Pilot cone area	[mm²]
$A_{Cone}(x_{Cone})$	Pilot cone area, dependent on position	[mm²]
$A_{Control}$	Control piston area	[mm²]
$A_{C,\ Piston}$	Pressure compensator piston area	[mm²]
$A_{MO}(x_{MO})$	Measuring orifice area, dependent on position	[mm²]
A_{Pilot}	Control piston area	[mm²]
A_{Ring}	Control piston area	[mm²]
$C_{H,A}$	Hydraulic system capacity	[l/bar]
C_c	Pressure compensator spring stiffness	[N/mm]
F_{Brake}	Brake force	[N]
F_{Flow}	Flow force	[N]
$F_{Solenoid}$	Solenoid force	[N]
F_{Spring}	Spring force	[N]
p_A, $\dot{p}_A$, $\ddot{p}_A$	Brake actuator piston side pressure and time derivatives	[bar, bar/s, bar/s²]
p_B, $\dot{p}_B$, $\ddot{p}_B$	Brake actuator ring side pressure and time derivatives	[bar, bar/s, bar/s²]
p_C	Pressure compensator pressure	[bar]
$p_{Control}$	Pressure after measuring orifice	[bar]
p_i	Pressures in valve test assembly	[bar]
p_{In}	Inlet pressure	[bar]
p_{Out}	Outlet pressure	[bar]
p_{Pilot}	Pilot pressure	[bar]
Q	Volume flow	[l/min]
Q_{BA}	Flow due to brake actuator motion	[l/min]
Q_C	Flow through pressure compensator	[l/min]
Q_{MO}	Flow through measuring orifice	[l/min]
Q_V, Q_{Valve}	Valve volume flow	[l/min]
r	Radius of holes	[mm]
$t_{a,e}$	Adjustment time, end	[s]
$t_{a,s}$	Adjustment time, start	[s]
$t_{d,e}$	Delay time, end	[s]
$t_{d,s}$	Delay time, start	[s]
x_C	Pressure compensator position	[mm]
$\dot{x}_{Fluid}$	Fluid velocity	[m/s]
x_{MO}	Measuring orifice position	[mm]
z	Number of holes	[-]
$\alpha_{D,C}$	Pressure compensator flow rate coefficient	[-]
$\alpha_{D,MO}$	Measuring orifice flow rate coefficient	[-]
Δp	Pressure difference	[bar]
ε	Flow angle	[°]
μ	Friction coefficient	[-]
ρ	Fluid density	[kg/m³]

References

Ewald, J., **Liermann, M.**, **Stammen, C.** and **Murrenhoff, H.** 2008. Application of Proportional Seat Valves to a Self-energising Electro Hydraulic Brake. In Proceedings of the *Symposium on Power Transmission and Motion Control*, September 10-12 2008, Bath, England.

Ewald, J. 2011. *Selbstverstärkende Elektro-Hydraulische Bremse (SEHB) für Schienenfahrzeuge*. Dissertation. RWTH Aachen University, Shaker, Aachen, Germany.

Hommen, W. 1986. Hydraulikbremse für Fahrzeuge, insbesondere Schienenfahrzeuge. *European Patent* No. EP0183089A1.

Kuehnlein, M., **Ewald, J.**, **Murrenhoff, H.** and **Liermann, M.** 2011. Non-linear Control and Observer Design for the Self-energizing Electro-Hydraulic Brake. In Proceedings of the *52nd National Conference on Fluid Power*, March 23-25 2011, Omnipress, Madison, Wisconsin, USA.

Liermann, M. 2008. *Self-energizing Electro-Hydraulic Brake*. Dissertation. RWTH Aachen University, Shaker, Aachen, Germany.

Linden, D. 2007. Das All-In-One-Ventil. O+P Ölhydraulik und Pneumatik 05/2007, pp. 261 - 263.

Murrenhoff, H. 2011. *Grundlagen der Fluidtechnik – Teil 1: Hydraulik*. Lecture Notes, Shaker, Aachen, Germany.

N.N. BS EN 13452-1:2003. 2003. Railway Applications – Braking – Mass transit brake systems. *British Railway Standard*, British Standards Institution.

N.N. ISO 6403 (1992-02-01). 1992. Hydraulic fluid power – Valves controlling flow and pressure – Test methods. *International Standard*, International Organization for Standardization.

N.N. Sterling Hydraulics. GS02 74. *Product Data Sheet*, http://www.sterling-hydraulics.com/files/pdf/gs02_70_71_74.pdf, visited on October 17, 2011.

Roth, H. 2010. Stromregelventil mit Proportional-Drosselventil und nachgeschalteter Druckwaage. *Swiss Patent* No. CH699508A1.

Schmidt, M. 2010. *Dichtheit als Entwicklungsschwerpunkt für Sitzventile hochdynamisch schaltender Zylinderantriebe*. Dissertation. RWTH Aachen University, Shaker, Aachen, Germany.

Trudzinski, M. 1980. *Experimentelle und analytische Bestimmung des Betriebsverhaltens von direktwirkenden und vorgesteuerten 2-Wege-Stromregelventilen*. Dissertation. TH Aachen.

Michael Kuehnlein
He received his Dipl.-Ing. in Mechanical Engineering from RWTH Aachen University, Germany in 2009. Since 2009 he is with the Institute for Fluid Power Drives and Controls (IFAS) at the same university. His research focus is on the Self-energising Electro-Hydraulic Brake and includes non-linear control.

Matthias Liermann
He received his Dipl.-Ing. in Mechanical Engineering from RWTH Aachen University, Germany in 2004. From 2004 until 2009 he was with IFAS. He received his PhD from RWTH Aachen University in 2008. Since 2009 he is Assistant Professor at the American University of Beirut (AUB), Beirut, Lebanon where he teaches control and automation.

Julian Ewald
He received his Dipl.-Ing. in Mechanical Engineering from RWTH Aachen University, Germany in 2007. He received his PhD from RWTH Aachen University in 2011. Since 2007 he is with IFAS. Since 2010 he is group leader “System and Control Technology”. His research focus is on the Self-energising Electro-Hydraulic Brake.

Hubertus Murrenhoff
He received his Dipl.-Ing. and PhD degree in Mechanical Engineering from RWTH Aachen University, Germany. From 1978 until 1986 he was with the Institute of Hydraulic and Pneumatic Drives (IHP). After eight years in industry as of October 1994 he is Executive Director of the Institute for Fluid Power Drives and Controls (IFAS) in conjunction with the corresponding chair at RWTH Aachen University, Germany. The renamed Institute IFAS was the former IHP headed by Professor Backé until 1994. Besides other involvements since 1999 he is Chairman of the Board of ‘Network of Fluid Power Centres in Europe‘ (FPCE).